Available online at www.sciencedirect.com
ScienceDirect
Communications in Nonlinear Science and Numerical Simulation 14 (2009) 473–488
Communications in Nonlinear Science and Numerical Simulation
www.elsevier.com/locate/cnsns

MHD flows of UCM fluids above porous stretching sheets using two-auxiliary-parameter homotopy analysis method

Amir Alizadeh-Pahlavan, Vahid Aliakbar, Farzad Vakili-Farahani, Kayvan Sadeghy *

University of Tehran, Department of Mechanical Engineering, P.O. Box 11155-4563, Tehran, Iran

Received 28 May 2007; received in revised form 24 September 2007; accepted 30 September 2007
Available online 9 October 2007

Abstract

The performance of a two-auxiliary-parameter homotopy analysis method (HAM) is investigated in solving laminar MHD flow of an upper-convected Maxwell fluid (UCM) above a porous isothermal stretching sheet. The analysis is carried out up to the 20th-order of approximation, and the effect of parameters such as elasticity number, suction/injection velocity, and magnetic number are studied on the velocity field above the sheet. The results will be contrasted with those reported recently by Hayat et al. [Hayat T, Abbas Z, Sajid M. Series solution for the upper-convected Maxwell fluid over a porous stretching plate. Phys Lett A 358;2006:396–403] obtained using a third-order one-auxiliary-parameter homotopy analysis method. It is concluded that the flow reversal phenomenon as predicted by Hayat et al. (2006) may have arisen because of the inadequacies of using just one-auxiliary-parameter in their analysis. That is, no flow reversal is predicted to occur if instead of using one-auxiliary-parameter use is made of two auxiliary parameters together with a more convenient set of base functions to assure the convergence of the series used to solve the highly nonlinear ODE governing the flow.

PACS: 47.50. −d

Keywords: Homotopy analysis method; MHD flow; UCM fluid; Porous stretching sheet

1. Introduction

Sheet stretching is an important operation in polymer industry [1]. Production of plastic sheets and foils, for example, involves extrusion of molten polymers through a slit die with the extrudate collected by a wind-up roll upon solidification. This process is normally accompanied with both heat and momentum transfer aspects. But there are also cases in which a plastic sheet may be stretched with no heat transfer involved. Cold drawing of plastic sheets, for example, is an important operation in which a plastic sheet is elongated in certain direction(s) in order to improve its mechanical properties in that direction(s) [2–4]. In all such operations (with or

* Corresponding author. Fax: +98 21 8801 3029.
E-mail address: sadeghy@ut.ac.ir (K. Sadeghy).

1007-5704/$ - see front matter
doi:10.1016/j.cnsns.2007.09.011

without heat transfer involved) the force required to pull the sheet is one of the most important design criteria. This force is known to depend to a large extent on the extensional viscosity of the sheet material. It also depends on the physical/rheological properties of the fluid surrounding the sheet. While traditionally Newtonian fluids are used for this purpose (e.g., water or air), but, in recent years it has been shown that there might be some advantages (particularly in flows involving heat transfer [5]) if the fluid surrounding the sheet can be made viscoelastic, say through the use of polymeric additives [6]. Alternatively, one may resort to injection or suction in order to modify flow kinematics provided the sheet is porous at the first place [7]. And in cases where the fluid surrounding the sheet is electrically-conducting, one may equally well rely on applying a sufficiently strong magnetic field to modify flow kinematics [8,9]. Conceivably, one might also envisage cases in which a combination of all these methods might be involved simultaneously to achieve the best result [10].

Among the techniques mentioned above to control flow kinematics, the idea of using magnetic fields appears to be the most attractive one both because of its ease of implementation and also because of its non-intrusive nature. The idea is not new and has shown its effectiveness for both Newtonian and non-Newtonian fluids alike [11–16]. There have been extensive efforts in the past, in both theoretical and experimental areas alike, to better understand such magnetohydrodynamic (MHD) flows. For Newtonian fluids, theoretical results are in favor of the experimental observations. For non-Newtonian fluids, in contrast, theoretical results are not always in support of experimental findings. This is not surprising realizing the fact that most studies carried out in the past on MHD flows of non-Newtonian fluids were concerned primarily with simple rheological models such as second-order model, or third-order model at best [5]. And this has been the case irrespective of the fact that these widely-used rheological models are known to violate certain thermodynamical constraints [17,18]. To this should be added the fact that these simple rheological models are known to be good only for fluids of low-elasticity in slow and/or slowly-varying flows. In practice, however, such restrictive conditions may not prevail. For reasons like these, the reliability of theoretical results obtained using such simple rheological models are in serious doubt.

In an interesting work carried out recently, Hayat et al. [19] tried to investigate MHD flow of a more realistic viscoelastic fluid model, i.e., the so-called upper-convected Maxwell model, above a porous stretching sheet. In an attempt to figure out the combined effects of parameters such as suction/injection velocity, fluid's elasticity, and the strength of the magnetic field on the flow kinematics and wall shear stress distribution, Hayat et al. [19] made use of a boundary layer formulation derived recently for this particular fluid model by Sadeghy et al. [20]. In order to obtain an analytical solution valid at large elasticity and/or magnetic numbers, they decided to rely on the homotopy analysis method. Restricting their analysis up to the third-order, Hayat et al. [19] concluded that by an increase in the elasticity number, the boundary layer becomes thinner and thinner. More importantly, they concluded that by an increase in the elasticity number the wall shear stress becomes progressively larger. An increase in the magnetic number was found to have similar effects on the boundary layer thickness and the wall shear stress distribution. These predictions, if true, are undoubtedly of significant industrial importance. However, there are currently no experimental data in the open literature to corroborate the significance of any of these predictions.

The work carried out by Hayat et al. [19] is obviously a major step towards understanding the role played by magnetic fields on the flow of viscoelastic fluids above stretching sheets. Having said this, it should be conceded that there are some intriguing results in their work which merit further investigation. For example, their Figs. 2, 6, and 10 (see Ref. [19]) show that a reverse flow is occurring above the sheet for the suction case. This interesting but rather puzzling prediction has not been scrutinized by Hayat et al. [19]. In the present work, it will be shown that such peculiar predictions have no basis on physical grounds. In fact, it will be shown that this unrealistic prediction may have roots in the use of an inappropriate auxiliary parameter in the HAM analysis as used by Hayat et al. [19]. We will show that when using homotopy analysis method to solve fluid mechanics problems dealing with the flow of viscoelastic fluids at high elasticity and/or magnetic numbers, it might be advisable to rely on two auxiliary parameters instead of one in the analysis.

2. Mathematical formulation

In this section, we briefly introduce the equations governing the laminar, two-dimensional flow induced in an otherwise quiescent, incompressible, electrically-conducting UCM fluid resting above a linearly-stretched

sheet. Starting from Cauchy equations of motion (which must include a source term due to the imposed magnetic field) use will be made of the boundary layer approximation to simplify the equations of motion. Following the same line as drawn by Sadeghy et al. [20] and Hayat et al. [19], the single partial differential equation governing the flow is turned out to be

$$u\frac{\partial u}{\partial x}+v\frac{\partial u}{\partial y}+\beta\left[u^2\left(\frac{\partial^2 u}{\partial x^2}\right)+v^2\left(\frac{\partial^2 u}{\partial y^2}\right)+2uv\left(\frac{\partial^2 u}{\partial x\,\partial y}\right)\right]=v\left(\frac{\partial^2 u}{\partial y^2}\right)-\frac{\sigma B_0^2}{\rho}u \tag{1}$$

where B_0 is the strength of the magnetic field, v is the kinematic viscosity of the fluid, and β is the relaxation time of the fluid. As to the boundary conditions, like Hayat et al. [19] we are going to assume that the sheet is being stretched linearly although it should be stressed that this is not necessarily the best scheme in the cold drawing operation of plastic sheets:

$$@y=0;\quad u=bx,\quad v=-V_s \tag{2}$$

$$@y\to\infty;\quad u\to 0 \tag{3}$$

In these relationships, b is a known constant and V_s is the suction/injection velocity (taken to be positive for the suction and negative for the injection). Eq. (1) combined with the continuity equation for an incompressible fluid, i.e., $\partial u/\partial x+\partial u/\partial y=0$, constitute the two equations governing the transfer of momentum between a stretching sheet and the fluid surrounding it. Now, since the flow is two-dimensional, use can be made of the concept of the stream function ψ to combine the momentum and continuity equations into a single partial differential equation in terms of ψ. The single PDE obtained this way can be transformed into an equivalent ODE using the technique of the similarity solution. Hayat et al. [19] introduced the following similarity parameter, η, and dimensionless stream function $f(\eta)$ for this purpose:

$$\eta=y\sqrt{\frac{b}{v}};\quad \psi=x\sqrt{vb}f(\eta) \tag{4}$$

The single ODE which is obtained this way is (see Refs. [19,20] for more details):

$$f'''-\mathbf{M}^2f'-f'^2+ff''+K(2ff'f''-f^2f''')=0 \tag{5}$$

where $M^2=\sigma B_0^2/\rho b$ is the magnetic number and $K=\beta b$ is the elasticity number. Eq. (5) is a third-order nonlinear ODE which requires three boundary conditions to be amenable to an analytical/numerical solution. In terms of f the required boundary conditions are

$$@\eta=0;f'=1;\quad f=R \tag{6}$$

$$@\eta\to\infty;\quad f'\to 0 \tag{7}$$

where $R=V_s/\sqrt{vb}$ is the dimensionless suction/injection velocity.

3. Method of solution

Eq. (5) with its pertinent boundary conditions, Eqs. (6) and (7), look too formidable to render themselves to a closed-form analytical solution. An approximate analytical solution could be obtained using the perturbation theory if it was given that K, M, or even R are sufficiently small. Obviously, one is always left with the option to solve this equation numerically, say using spectral methods. In the present work, like Hayat et al. [19], we have decided to rely on the HAM to obtain an analytical solution with the advantage that such a solution, if it can be found, is valid even at large elasticity or magnetic numbers [21–24]. It is worth mentioning that the method has recently been applied to many fluid mechanics problems for Newtonian and non-Newtonian fluids alike [25–38].

The basic idea in applying the HAM, as described in detail by Liao in Ref. [24], is to assume that the solution can be written as a series in terms of certain base functions. We have found it appropriate to use the following base functions for this purpose:

$$f(\eta)=\sum_{m=0}^{\infty}\sum_{n=0}^{\infty}a_{m,n}\mathrm{e}^{-n\lambda\eta} \tag{8}$$

The above series is seen to satisfy the boundary condition at infinity. And it will be constructed in such a way that it converges to the exact analytical solution provided that sufficient number of terms is used in the series. The problem then becomes how to adjust the parameter λ and the coefficients $a_{m,\,n}$ such that the proposed solution satisfies both the governing equation (Eq. (5)) and the remaining boundary conditions at $\eta = 0$. To achieve this goal, we make an initial guess on $f(\eta)$ such that it satisfies the boundary condition at $\eta = 0$ and at the same time complies with the *Rule of Solution Expression* as required in the homotopy analysis method (see Ref. [24] for more details); that is

$$f_0(\eta) = R + \frac{1}{\lambda}(1 - \mathrm{e}^{-\lambda\eta}) \tag{9}$$

It is to be noted that for reasons which will be made clear shortly, our proposed series solution for f (see Eq. (8)) and also our initial guess for f_0 (see Eq. (9)) differ from those used by Hayat et al. [19] by the presence of an extra auxiliary parameter λ (see Ref. [24] for the details). We have also relied on a different set of base functions with better convergence properties as compared to the base functions used by Hayat et al. [19]. Now, following a line similar to that drawn by Liao [24], and Hayat et al. [19] we introduce an auxiliary linear operator in the form,

$$L(f) = f''' + \lambda f'' \tag{10}$$

It is easy to check that this operator satisfies the following equation:

$$L\left[\frac{C_1\mathrm{e}^{-\lambda\eta}}{\lambda^2} + C_2\eta + C_3\right] = 0 \tag{11}$$

where C_1, C_2, and C_3 are arbitrary constants. On the basis of the governing equation itself, Eq. (5), we introduce the following nonlinear operator $\Im$:

$$\begin{aligned}\Im[F(\eta;q)] = {} & \frac{\partial^3 F(\eta;q)}{\partial\eta^3} - M^2\frac{\partial F(\eta;q)}{\partial\eta} - \left(\frac{\partial F(\eta;q)}{\partial\eta}\right)^2 + F(\eta;q)\frac{\partial^2 F(\eta;q)}{\partial\eta^2} \\ & + K\left\{2F(\eta;q)\frac{\partial F(\eta;q)}{\partial\eta}\frac{\partial^2 F(\eta;q)}{\partial\eta^2} - (F(\eta;q))^2\frac{\partial^3 F(\eta;q)}{\partial\eta^3}\right\}\end{aligned} \tag{12}$$

where $F(\eta; q)$ is a kind of mapping function for $f(\eta)$ with q serving as an embedding parameter being in the range of [0, 1]. Using these operators, we construct the so-called zero-order deformation equation as

$$(1-q)L[F(\eta;q) - f_0(\eta)] = q\hbar H(\eta)\Im[F(\eta;q)] \tag{13}$$

where $\hbar$ is an auxiliary parameter (the same as that introduced by Hayat et al. [19]) with $H(\eta)$ being a new auxiliary function. The boundary conditions for this equation are

$$\begin{cases} F(0;q) = R \\ F'(0;q) = 1 \\ F'(\infty;q) = 0 \end{cases} \tag{14}$$

It is to be noted that our zero-order equation, Eq. (13), contains an extra auxiliary function $H(\eta)$ which does not exist in its counterpart as used by Hayat et al. [19]. It is easy to check that for $q = 0$ the above system of equations has the trivial solution of $F(\eta; 0) = f_0(\eta)$. And for $q = 1$, it is equivalent to the original differential equation (Eq. (5)) provided that we have $F(\eta; 1) = f(\eta)$. Thus, as q increases from 0 to 1, the mapping function $F(\eta; q)$ varies from the initial guess, $f_0(\eta)$ to the final yet unknown solution $f(\eta)$. Now expanding $F(\eta; q)$ by its Taylor series in terms of q, one would obtain

$$F(\eta;q) = f_0(\eta) + \sum_{m=1}^{\infty} f_m(\eta)q^m \tag{15}$$

where

$$f_m(\eta) = \frac{1}{m!}\left.\frac{\partial^m F(\eta;q)}{\partial q^m}\right|_{q=0} \tag{16}$$

For the above series to converge at $q = 1$, the auxiliary linear operator L, the auxiliary function $H(\eta)$, and the auxiliary parameters $\hbar$ and λ have to be chosen appropriately. The final series solution then becomes

$$f(\eta) = f_0(\eta) + \sum_{m=1}^{\infty} f_m(\eta) \tag{17}$$

It is to be noted that at this stage in the analysis, $f_m(\eta)$ is still unknown. In order to obtain $f_m(\eta)$, we first differentiate the zero-order deformation equations m times with respect to q then divide the equation so obtained by $m!$ and finally set $q = 0$. With such maneuvering, the so-called high-order deformation equation is obtained for $f_m(\eta)$ as

$$L[f_m(\eta) - \chi_m f_{m-1}(\eta)] = \hbar H(\eta)\Re_m(\eta). \tag{18}$$

where we have

$$\chi_m = \begin{cases} 0, & m \leqslant 1 \\ 1, & m > 1 \end{cases} \tag{19}$$

and

$$\Re_m(\eta) = f'''_{m-1} - M^2 f'_{m-1} + \sum_{k=0}^{m-1}\left[f_{m-1-k}f''_k - f'_{m-1-k}f'_k + K f_{m-1-k}\sum_{l=0}^{k}\left\{2f'_{k-l}f''_l - f_{k-l}f'''_l\right\}\right] \tag{20}$$

The boundary conditions for Eq. (18) are

$$\begin{cases} f_m(0) = 0 \\ f'_m(0) = 0 \\ f'_m(\infty) = 0 \end{cases} \tag{21}$$

In an attempt to satisfy the *Rule of Solution Expression*, the *Rule of Coefficient Ergodicity*, and the *Rule of Solution Existence* as discussed by Liao [24], the auxiliary function $H(\eta)$ is chosen to be

$$H(\eta) = \mathrm{e}^{-\lambda\eta} \tag{22}$$

Having decided on the auxiliary function, it is quite easy to solve high-order deformation equations. To that end, let $f^*_m(\eta)$ denote a special solution for Eqs. (18) and (21). The general solution can then be written as

$$f_m(\eta) = f^*_m(\eta) + \frac{C'_1\mathrm{e}^{-\lambda\eta}}{\lambda^2} + C'_2\eta + C'_3 \tag{23}$$

where C'_1, C'_2 and C'_3 are constants of integration. To satisfy the boundary condition at infinity, i.e., $f'_m(\infty) = 0$, we should have $C'_2 = 0$. The remaining constants C'_1, C'_3 can be determined using the boundary conditions at $\eta = 0$. The symbolic software MATHEMATICA can be used to solve Eqs. (18) and (21). The final result becomes

$$f_m(\eta) = \sum_{n=0}^{3m+1} a_{m,n}\mathrm{e}^{-n\lambda\eta} \tag{24}$$

Substituting this relationship for $f_m(\eta)$ in the high-order deformation equation, the following recurrence formulas are obtained for the missing coefficients $a_{m,n}$:

$$a_{m,0} = \chi_m\chi_{3m}a_{m-1,0} + \sum_{n=2}^{3m+1}\frac{\Delta_{m,n-1}}{n^2\lambda^3}$$

$$a_{m,1} = \chi_m\chi_{3m-n}a_{m-1,1} - \sum_{n=2}^{3m+1}\frac{\Delta_{m,n-1}}{n(n-1)\lambda^3} \tag{25}$$

$$a_{m,n} = \chi_m\chi_{3m-n}a_{m-1,n} + \frac{\Delta_{m,n-1}}{n^2(n-1)\lambda^3} \tag{26}$$

where we have $2 \leqslant n \leqslant 3m+1$, and

$$\Delta_{m,n} = \eta[\chi_{3m-n} n\lambda\left(M^2 - n^2\lambda^2\right)a_{m-1,n} + \chi_{3m-n+1}\lambda^2 b_{m,n} + K\lambda^3 c_{m,n}] \tag{27}$$

In these equations, the coefficients $b_{m,n}$ and $c_{m,n}$ are defined as

$$b_{m,n} = \sum_{k=0}^{m-1} \sum_{i=\max\{0,n-3k-1\}}^{\min\{n,3(m-k)-2\}} (n-i)(n-2i)a_{m-k-1,i}a_{k,n-i} \tag{28}$$

$$c_{m,n} = \sum_{k=0}^{m-1} \sum_{l=0}^{k} \sum_{i=\max\{0,n-2k-2\}}^{\min\{n,3(m-k)+2\}} \sum_{q=\max\{0,n-3l-1\}}^{\min\{n,3(k-l)+1\}} -(n-i-q)^2(3q-n+i)a_{m-k-1,i}a_{k-l,q}a_{l,n-i-q} \tag{29}$$

where $m \geqslant 1$ and $0 \leqslant n \leqslant 3m+1$. Using these formulas we can calculate all coefficients $a_{m,n}$ knowing the first two coefficients $a_{0,0}$ and $a_{0,1}$ as

$$a_{0,0} = R + \frac{1}{\lambda}; \quad a_{0,1} = -\frac{1}{\lambda} \tag{30}$$

The end result is an explicit expression for the desired series solution provided that N is sufficiently large. That is

$$f(\eta) = \lim_{N\to\infty} \sum_{m=0}^{N} f_m(\eta) = \lim_{N\to\infty} \sum_{m=0}^{N} \sum_{n=0}^{3m+1} a_{m,n}\mathrm{e}^{-n\lambda\eta} \tag{31}$$

In practice, however, we decided to stop the calculations at $N = 20$ (i.e., at 20th-order) having realized that a sufficiently small tolerance has been met. This should be contrasted with the HAM as used by Hayat et al. [19] in which the analysis was extended up to the third-order only.

4. Results and discussion

The infinite series as given by Eq. (31) gives rise to a family of explicit analytic expressions in terms of the two adjusting parameters $\hbar$, λ. Obviously, not all members of this family necessarily converge to $f(\eta)$. In practice, some members of this family might even be "better" than others in terms of convergence. One thing good about the HAM is that it provides us with great flexibility to select the best values for $\hbar$, λ such that the series eventually converges to the desired solution $f(\eta)$. Obviously, if the series solution as represented by Eq. (31) is convergent at $\eta = 0$, its derivatives should also converge at $\eta = 0$; that is

$$f''(0) = \sum_{m=0}^{+\infty} f_m''(0), f'''(0) = \sum_{m=0}^{+\infty} f_m'''(0), \cdots \tag{32}$$

Our calculations indicate that Eq. (31) converges to $f(\eta)$ over the whole range of $[0, \infty]$ as long as the above derivative-equation is also convergent over the same domain. It is worth mentioning that different values of λ correspond to different initial guess, $f_0(\eta)$, and different linear operators, L. Similarly, different values of $\hbar$ correspond to different zero-order deformation equations. This means that, in practice, there are an infinite number of pairs of $\hbar$, λ which can make the series equation (31) to converge to the final *unique* solution. It also means that although the solution to the governing equation, Eq. (5), is *unique* but it can be expressed by an *infinite* number of expressions. Obviously, it is conceivable that some of these approaches might be better than others. In the present work we used different combinations of $\hbar$, λ to obtain converged results. To find the best values for $\hbar$, λ, as was pointed out by Liao [24] it is sufficient to plot the physical quantity which is represented by the original governing equation. In the present work, like Hayat et al. [19] we are going to plot the wall shear stress (as represented by $f''(0)$) for this purpose. As discussed by Liao [24], under converged conditions, when a physical quantity is plotted in terms of $\hbar$ or λ, a horizontal line segment should appear in the plot. This horizontal segment is commonly referred to as the *valid region*, and as long as we choose $\hbar$, λ in this region we can be sure that the series converges to its unique value.

With these ideas in mind, we have determined the *validity region* for both $\hbar$ and λ for any given combination of K, R, M by monitoring their effect on $f''(0)$. Figs. 1 and 2 show typical $\hbar$- and λ-curves obtained this way for the case where we have: $R = -0.3$, $K = 10$ and $M = 10$ for two different levels of approximations, i.e., 10th-order and 20th-order. A broad *valid region* is evident in these figures for both orders of approximations demonstrating that one can be assured of the convergence of the series solution used in this work. Fig. 3 shows that the size of the *valid region* strongly depends on the elasticity number K. In fact, it becomes shorter the higher the elasticity number. The strong influence of the elasticity number on the size of the *valid zone* is not surprising realizing the fact that it appears in the highly nonlinear term in the governing equation, Eq. (5). We have also plotted $\hbar$-curves using the third-order formulations as developed by Hayat et al. [19]. As shown in Fig. 4, the *valid region* is much shorter for Hayat et al. [19] case as compared to ours. In fact, our calculations show

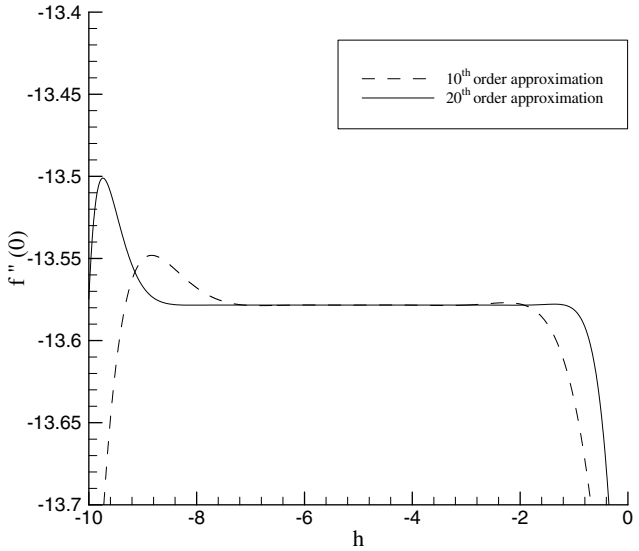

Fig. 1. $\hbar$-Curves for $R = -0.3$, $K = 10$, $M = 10$, $\lambda = 14$ for two different orders of approximation.

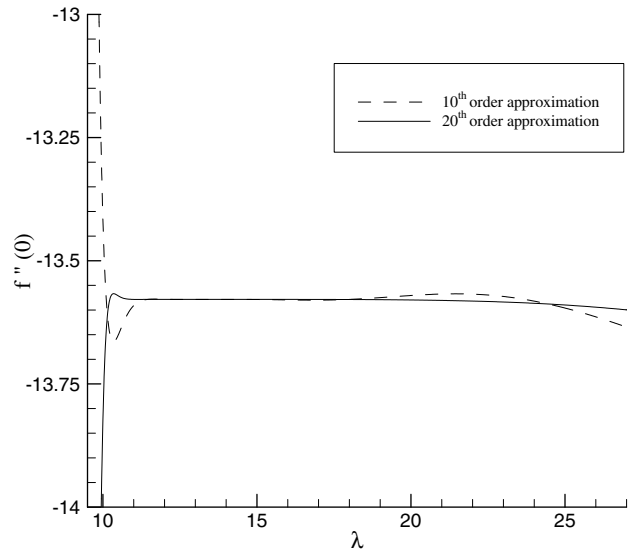

Fig. 2. λ-Curve for $R = -0.3$, $K = 10$, $M = 10$, $\hbar = -5$ for two different orders of approximation.

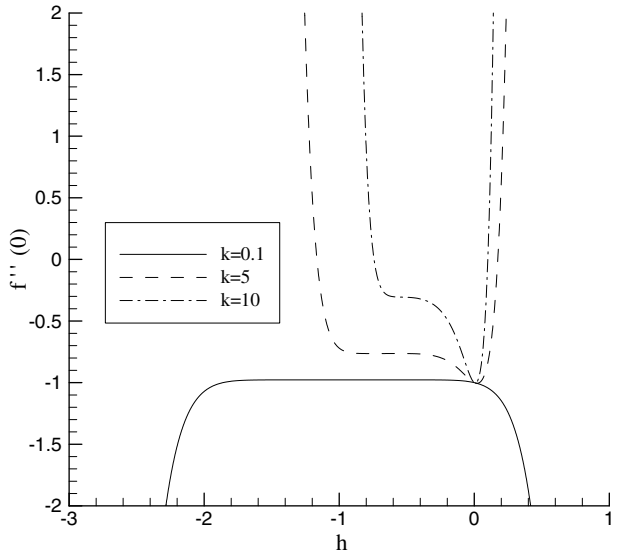

Fig. 3. The effect of the elasticity number K on the $\hbar$-curve for $R = -0.3$ and $M = 0.5$ without using λ as the second auxiliary parameter.

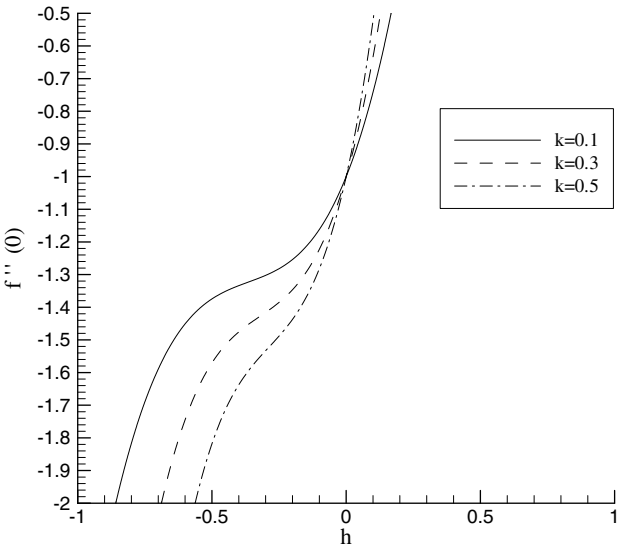

Fig. 4. The effect of the elasticity number K on the $\hbar$-curve for $R = 0.3$ and $M = 0.5$ obtained using Hayat's [19] one-parameter HAM.

that at sufficiently high elasticity numbers the convergence of their series solution is in serious doubt. As a matter of fact, by extending their analysis up to fourth-order we have noticed that their series solution diverges. It is obvious that using two adjusting auxiliary parameters instead of one parameter, as proposed in this work, gives rise to a wider *valid zone* thus guaranteeing the convergence of the series.

Having chosen the best values for $\hbar$ and λ (see Tables 1 and 2) for our two-parameter HAM, we are now at a stage to present the velocity profiles obtained in this work for different combinations of K, R, and M, and compare them with those reported by Hayat et al. [19]. Fig. 5 shows the effect of the suction/injection on the velocity profiles obtained using our two-parameter HAM. For comparison purposes we have reproduced Hayat's results and presented them in Fig. 6. A flow reversal is evident in Fig. 6 for the suction case in Hayat et al. work [19]. In contrast, our results in Fig. 5 do not show any reverse flow whatsoever. We have also calculated the effect of the suction/injection on the v-velocity component using both methods and found dramatic

Table 1
The effect of the elasticity number K on $f''(0)$ for the case of suction ($R = 0.3$ and $M = 0.5$)

K	λ	$\hbar$	δ	$f''(0)$
0	1.3	−1	3.574	−1.2784
1	1.9	−1.5	2.262	−1.9959
2	3	−1.5	1.509	−2.8712
3	4.5	−1.5	1.050	−3.9613
4	5.5	−2	0.826	−5.3171
5	7.5	−2	0.614	−7.1254
6	10	−2	0.460	−9.6214
7	14	−3	0.332	−13.338
8	20	−4	0.231	−19.402
9	32	−6	0.145	−31.212
10	65	−13	0.071	−64.224

Table 2
The effect of the elasticity number K on $f''(0)$ for the case of injection ($R = -0.3$ and $M = 0.5$)

K	λ	$\hbar$	δ	$f''(0)$
0	1	−1	4.66157	−0.978163
1	1.2	−1	3.91552	−0.962215
2	1.5	−1	3.31299	−0.930555
3	1.7	−1	2.98373	−0.885648
4	1.9	−1	2.72783	−0.830316
5	2	−1	2.59154	−0.76491
6	1.4	−1	2.85084	−0.690684
7	1.2	−1	2.73006	−0.609347
8	1.5	−1	2.61202	−0.519199
9	1.5	−1	2.51918	−0.420646
10	1.4	−1	2.42742	−0.311931

differences between their outputs. Results obtained using our two-parameter method, as presented in Fig. 7, are well-behaved inferring a kind of shift in the profiles whereas results obtained using Hayat's one-parameter method (see Fig. 8) show some peculiar behavior above the sheet. In our opinion, results obtained by Hayat

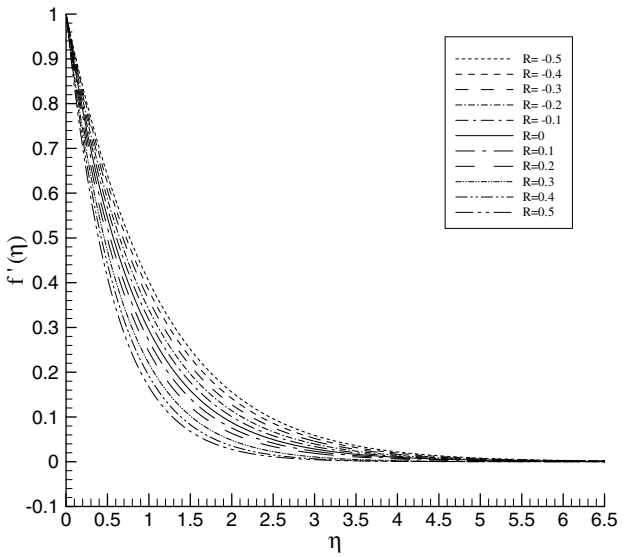

Fig. 5. The effect of the suction/injection number R on the u-velocity component obtained using our two-parameter HAM at $K = 0.3$ and $M = 0.5$.

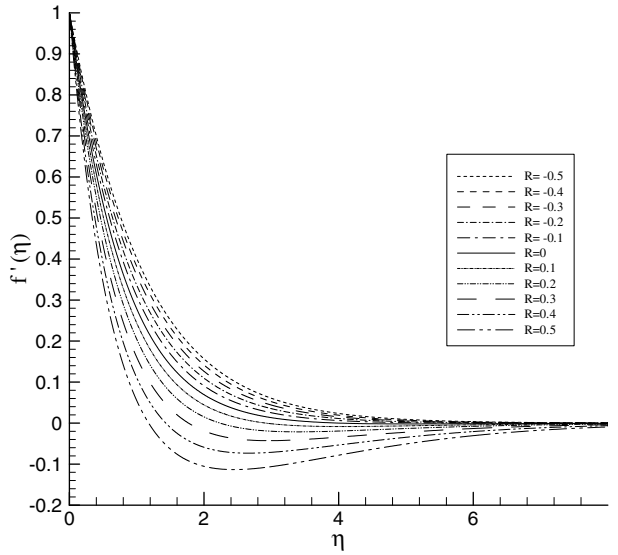

Fig. 6. The effect of the suction/injection number R on the u-velocity component obtained using Hayat's one-parameter HAM at $K = 0.3$ and $M = 0.5$.

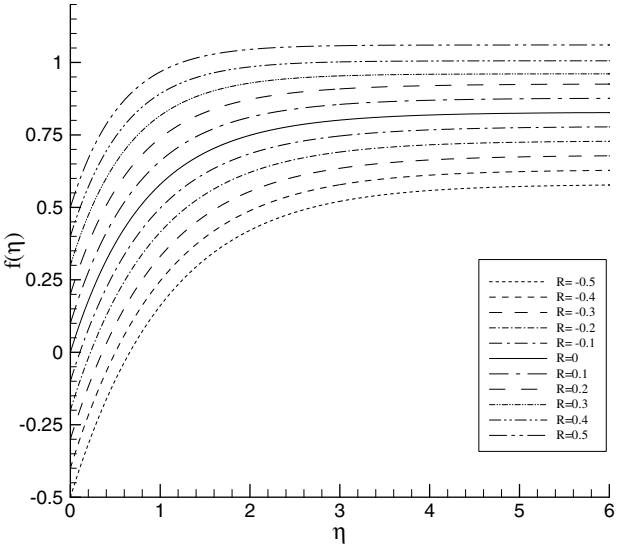

Fig. 7. The effect of the suction/injection number R on the v-velocity component obtained using our two-parameter HAM at $K = 0.3$ and $M = 0.5$.

et al. [19] are unrealistic lacking any physical explanation. That is, suction or injection should not be able to cause a backflow by themselves unless they are strong enough to induce an adverse pressure gradient above the sheet as required for flow reversal. But under such conditions the boundary layer formulations used for the analysis should be reworked because in its current form it has been assumed that there is no pressure gradient involved in the boundary layer. Indeed, our calculations show that the prediction of flow reversal for the suction case as obtained by Hayat et al. [19] can be traced back to assigning an inappropriate value to the auxiliary parameter $\hbar$. That is, an adoption of the same value for $\hbar$ (i.e., $\hbar = -0.5$) can be shown to be good for the injection case but not so good for the suction case, as far as series convergence is concerned. This is perhaps why Hayat et al. [19] did not attempt to extend their HAM to an order higher than three because their series simply would have diverged.

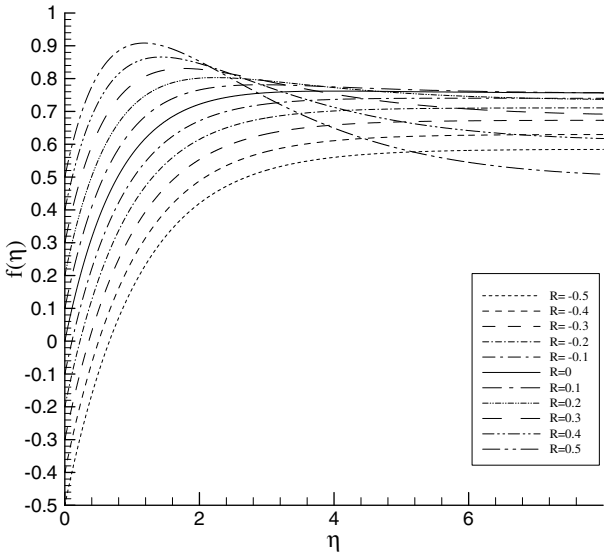

Fig. 8. The effect of the suction/injection number R on the v-velocity component obtained using Hayat's one-parameter HAM at $K = 0.3$ and $M = 0.5$.

The above arguments can also be used to explain the discrepancy which exists between our results and those reported by Hayat et al. [19] when addressing the effect of the elasticity and magnetic numbers on the velocity profiles. Fig. 9 shows the effect of the elasticity number on the velocity profiles obtained using our two-parameter HAM. And Fig. 10 presents a reproduction of Hayat's results. Again a flow reversal is noticeable in Hayat's results which do not exist in our results (see Fig. 9). The predictions of the two methods for the v-velocity component are also at odds (see Figs. 11 and 12). The same can be said about the effect of the magnetic field on the velocity profiles. For example, Figs. 13 and 15 show the effect of the magnetic number on the u and v velocity profiles obtained using our two-parameter HAM. Hayat's results have been presented in Figs.

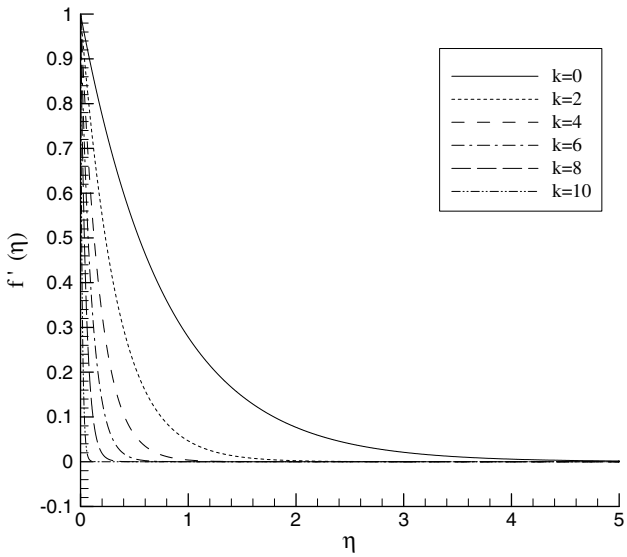

Fig. 9. The effect of the elasticity number K on the u-velocity component obtained using our two-parameter HAM at $R = 0.3$ and $M = 0.5$.

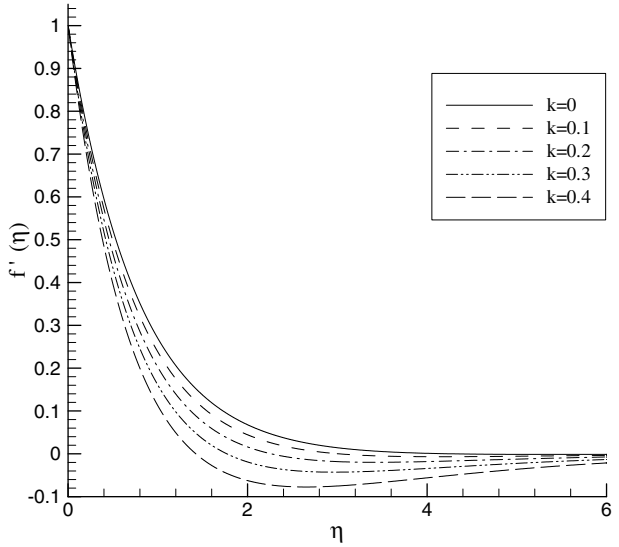

Fig. 10. The effect of the elasticity number K on the u-velocity component obtained using Hayat's one-parameter HAM at $R = 0.3$ and $M = 0.5$.

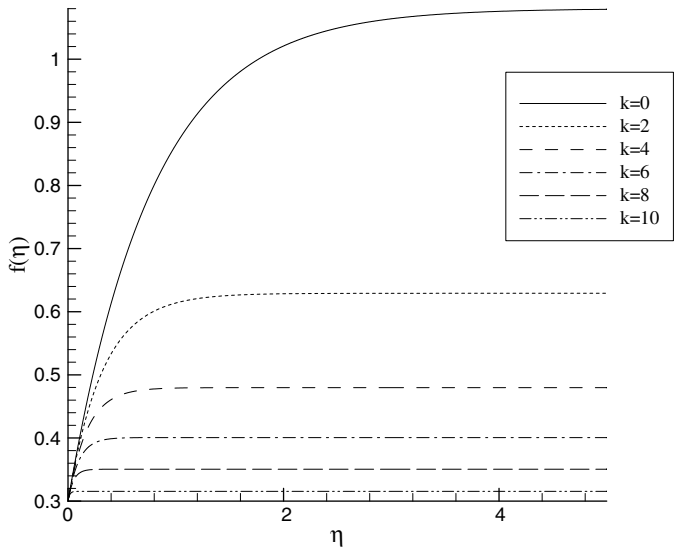

Fig. 11. The effect of the elasticity number K on the v-velocity component obtained using our two-parameter HAM at $R = 0.3$ and $M = 0.5$.

14 and 16. Obviously, our results do not show any flow reversal demonstrating the profound effect of the auxiliary parameter on the accuracy of the results obtained using HAM. That is, there are marked differences between the performance of the two-parameter HAM used in the present work with the one-parameter HAM used by Hayat et al. [19]. Having said this, it should be added that although there are quantitative differences between our results and those reported by Hayat et al. [19] as to the velocity profiles, but qualitatively, our results confirm the general conclusion made by Hayat et al. [19] that by an increase in the elasticity or magnetic number the wall shear stress, represented by $f''(0)$, is increased and the boundary layer thickness is decreased. Tables 1–4 show results for the wall shear stress and boundary layer thickness (δ). These tables also include the set of $\hbar$–λ values used in practice for the series to converge.

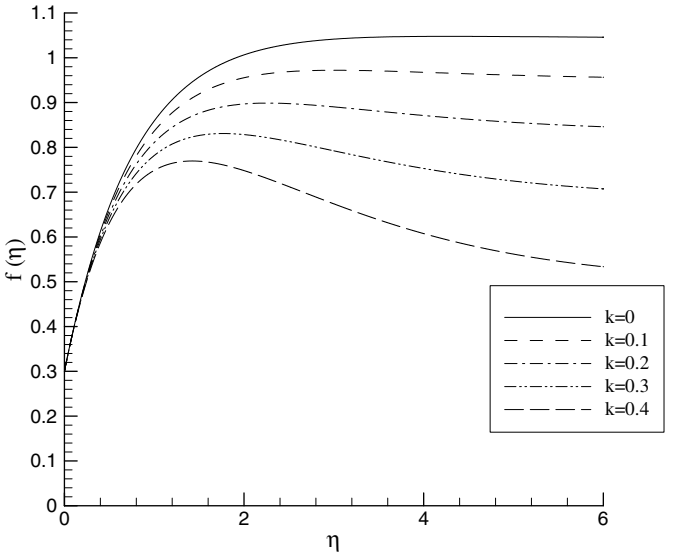

Fig. 12. The effect of the elasticity number K on the v-velocity component obtained using Hayat's one-parameter HAM at $R = 0.3$ and $M = 0.5$.

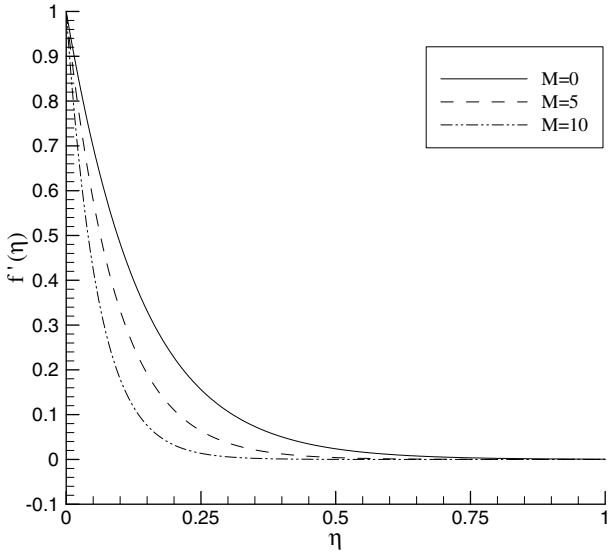

Fig. 13. The effect of the magnetic number M on the u-velocity component obtained using our two-parameter HAM at $R = 0.3$ and $K = 5$.

5. Concluding remarks

Based on the results obtained in the present work it can be concluded that in applying HAM to highly nonlinear equations such as those encountered in the flow of viscoelastic fluids, it might be advisable to base the analysis on two auxiliary parameters instead of one. It is also advisable that for each set of working parameters such as the elasticity number, the magnetic number, and the suction/injection number different values should be assigned to the auxiliary parameters to guarantee the convergence of the series. The marked difference which exists between the results of our two-parameter HAM and the results obtained by Hayat et al. [19] using one parameter HAM can be attributed to the fact that their series solution does not satisfy one of the

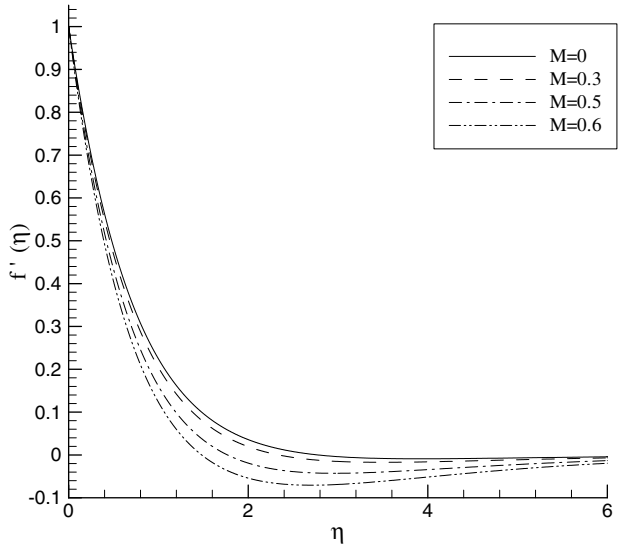

Fig. 14. The effect of the magnetic number M on the u-velocity component obtained using Hayat's one-parameter HAM at $R = 0.3$ and $K = 0.3$.

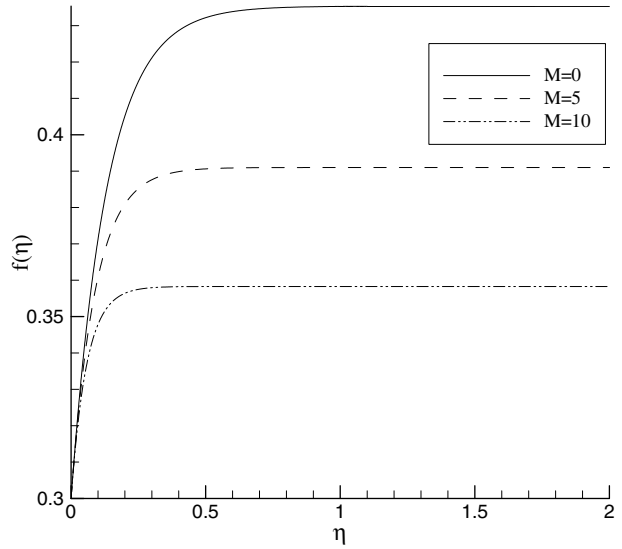

Fig. 15. The effect of the magnetic number M on the v-velocity component obtained using our two-parameter HAM at $R = 0.3$ and $K = 5$.

fundamental rules of the homotopy analysis method, i.e., the "Rule of Coefficient Ergodicity". Based on this rule, as the order of the approximation is increased, all terms of the base functions should appear in the solution expression, and each coefficient should be modified accordingly. But in the series solution as used by Hayat et al. [19], the term $e^{-2\eta}$ always disappears thus violating this basic rule. To this should be added the fact that in the HAM (provided the series is convergent) one should obtain more accurate results by simply increasing the order of the approximation. But because of the shortcomings mentioned above, increasing the order of the approximation from thee to four makes the series used by Hayat et al. [19] to diverge. This is perhaps why their HAM was cut off at a low order of just three. This should be contrasted with the present work in which we could easily obtain converged results up to an order of 20.

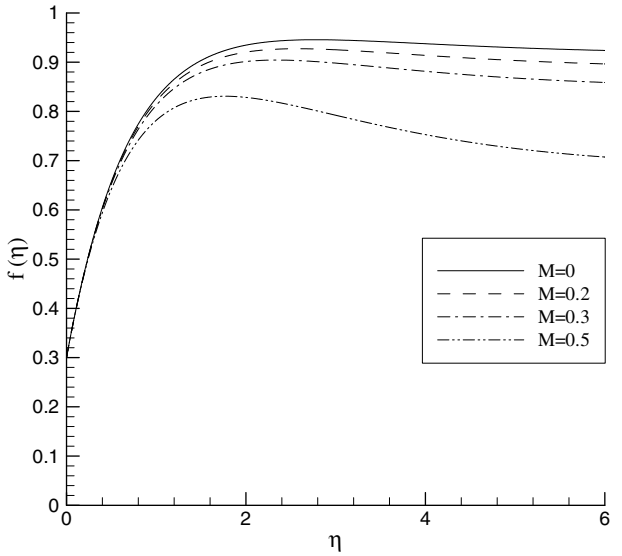

Fig. 16. The effect of the magnetic number M on the v-velocity component obtained using Hayat's one-parameter HAM at $R = 0.3$ and $K = 0.3$.

Table 3
The effect of the magnetic number M on $f''(0)$ for the case of suction ($R = 0.3$)

K	M	λ	$\hbar$	δ	$f''(0)$
0	0	1	−1	4.221	−1.1589
	5	5.2	−1	0.881	−5.25119
	10	10.2	−1	0.452	−10.201
5	0	7.5	−2	0.616	−7.0737
	5	10.9	−2	0.42	−10.8399
	10	17.2	−2	0.268	−17.0558
10	0	65	−13	0.071	−64.1885
	5	68.3	−11	0.068	−67.7827
	10	77.4	−13	0.06	−76.9326

Table 4
The effect of the magnetic number M on $f''(0)$ for the case of injection ($R = -0.3$)

K	M	λ	$\hbar$	δ	$f''(0)$
0	0	0.9	−1	5.23483	−0.861506
	5	5	−1	0.926576	−4.95122
	10	9.9	−1	0.46514	−9.901
5	0	1.6	−1	2.90135	−0.700263
	5	5	−1.5	0.917446	−4.74886
	10	11.1	−1.8	0.413072	−11.0275
10	0	1.4	−1	2.46289	−0.269701
	5	4.9	−3	0.909802	−4.15231
	10	14	−5	0.325586	−13.5784

Acknowledgements

The authors would like to thank Research Council of the University of Tehran for supporting this work. Thanks are also due to the reviewer(s) for their constructive comments which have contributed profoundly to the quality of the final work.

References

[1] Agassant JF, Avens P, Sergent J, Carreau PJ. Polymer, processing: principles and modeling. Munich: Hanser Publishers; 1991.
[2] Lazurkin JS. Cold-drawing of glass-like and crystalline polymers. J Polym Sci 1958;30(121):595–604.
[3] Ginzburg BM. On the cold drawing of semicrystalline polymers. J Macromol Sci Part B 2005;44(2):217–23.
[4] Casas F, Alba-Simionesco C, Lequeux F, Montès H. Cold drawing of polymers: plasticity and aging. J Non-Crystal Solids 2006;352(42–49):5076–80.
[5] Bird RB, Armstrong RC, Hassager O. Dynamics of polymeric liquids, vols. I and II. New York: Wiley; 1987.
[6] Dandapat BS, Gupta AS. Flow and heat transfer in a viscoelastic fluid over a stretching sheet. Int J Non-Linear Mech 1989;24(3):215–9.
[7] Subhas A, Veena P. Viscoelastic fluid flow and heat transfer in a porous medium over a stretching sheet. Int J Non-Linear Mech 1998;33(3):531–40.
[8] Cortell R. A note on magnetohydrodynamic flow of a power-law fluid over a stretching sheet. Appl Math Comput 2005;168:557–66.
[9] Cortell R. Effects of viscous dissipation and work done by deformation on the MHD flow and heat transfer of a viscoelastic fluid over a stretching sheet. Phys Lett A 2006;357:298–305.
[10] Cortell R. Flow and heat transfer of an electrically-conducting fluid of second grade over a stretching sheet subject to suction and to a transverse magnetic field. Int J Heat Mass Transfer 2006;49:1851–6.
[11] Hayat T, Khan M, Asghar S. Magnetohydrodynamic flow of an Oldroyd 6-constant fluid. Appl Math Comput 2004;155:417–25.
[12] Chakrabarti A, Gupta AS. Hydromagnetic flow heat and mass transfer over a stretching sheet. Quart Appl Math 1973;37:73–8.
[13] Kandasamy R, Periasamy K, Sivagnana Prabhu KK. Chemical reaction, heat and mass transfer on MHD flow over a vertical stretching surface with heat source and thermal stratification effects. Int J Heat Mass Transfer 2005;48:4557–61.
[14] Chung-Liu I. Flow and heat transfer of an electrically-conducting fluid of second grade in a porous medium over a stretching sheet subject to a transverse magnetic field. Int J Non-Linear Mech 2005;40:465–74.
[15] Takhar HS, Chamkha AJ, Nath G. Flow and mass transfer on a stretching sheet with a magnetic field and chemically reactive species. Int J Eng Sci 2003;38:1303–14.
[16] Chung-Liu I. A note on heat and mass transfer for a hydromagnetic flow over a stretching sheet. Int Commun Heat Mass Transfer 2005;32:1075–84.
[17] Fosdick RL, Rajagopal KR. Anomalous features in the model of second-order fluids. Arch Ration Mech Anal 1979;70:689.
[18] Dunn JE, Rajagopal KR. Fluids of differential type: critical review and thermodynamic analysis. Int J Eng Sci 1995;33:689.
[19] Hayat T, Abbas Z, Sajid M. Series solution for the upper-convected Maxwell fluid over a porous stretching plate. Phys Lett A 2006;358:396–403.
[20] Sadeghy K, Najafi AH, Saffaripour M. Sakiadis flow of an upper-convected Maxwell fluid. Int J Non-Linear Mech 2005;40:1220–8.
[21] Hilton PJ. An introduction to homotopy theory. Cambridge University Press; 1953.
[22] Alexander JC, Yorke JA. The homotopy continuation method: numerically implementable topological procedures. Trans Am Math Soc 1978;242:271–84.
[23] Grigolyuk EI, Shalashilin VI. Problems of nonlinear deformation: the continuation method applied to nonlinear problems in solid mechanics. Dordrecht, Hardbound: Kluwer Academic Publishers; 1991.
[24] Liao SJ. Beyond perturbation: introduction to homotopy analysis method. Boca Raton: Chapman & Hall/CRC Press; 2003.
[25] Liao SJ. A uniformly valid analytic solution of 2D viscous flow past a semi-infinite flat plate. J Fluid Mech 1999;385:101–28.
[26] Liao SJ. On the analytic solution of magnetohydrodynamic flows of non-Newtonian fluids over a stretching sheet. J Fluid Mech 2003;488:189–212.
[27] Liao SJ. On the homotopy analysis method for nonlinear problems. Appl Math Comput 2004;147:499–513.
[28] Liao SJ. A new branch of solutions of boundary-layer flows over an impermeable stretched plate. Int J Heat Mass Transfer 2005;48(12):2529–39.
[29] Liao SJ. An analytic solution of unsteady boundary-layer flows caused by an impulsively stretching plate. Commun Nonlinear Sci Numer Simul 2006;11(3):326–39.
[30] Liao SJ, Campo A. Analytic solutions of the temperature distribution in Blasius viscous flow problems. J Fluid Mech 2002;453:411–25.
[31] Liao SJ, Pop I. Explicit analytic solution for similarity boundary layer equations. Int J Heat Mass Transfer 2004;47(1):75–85.
[32] Xu H, Liao SJ. Analytic solutions of magnetohydrodynamic flows of non-Newtonian fluids caused by an impulsively stretching plate. J Non-Newton Fluid Mech 2005;129:46–55.
[33] Ayub M, Rasheed A, Hayat T. Exact flow of a third grade fluid past a porous plate using homotopy analysis method. Int J Eng Sci 2003;41:2091–103.
[34] Hayat T, Khan M, Asghar S. Homotopy analysis of MHD flows of an Oldroyd 8-constant fluid. Acta Mech 2004;168:213–32.
[35] Hayat T, Khan M, Ayub M. On the explicit analytic solutions of an Oldroyd 6-constant fluid. Int J Eng Sci 2004;42:123–35.
[36] Hayat T, Sajid M. On analytic solution for thin film flow of a fourth grade fluid down a vertical cylinder. Phys Lett A 2007;361:316–22.
[37] Mustafa Inc.. On exact solution of Laplace equation with Dirichlet and Neumann boundary conditions by the homotopy analysis method. Phys Lett A 2007;365:412–5.
[38] Mhone PY, Makinde OD. Unsteady MHD flow with heat transfer in a diverging channel. Romanian J Phys 2006;51(9–10):963–75.